

# Phase Sensitive Reconstruction in Diffusion Spectrum Imaging Enabling Velocity Encoding and Unbiased Noise Distribution

Jonathan I. Sperl<sup>1</sup>, Ek T. Tan<sup>2</sup>, Tim Sprenger<sup>1,3</sup>, Vladimir Golkov<sup>1,3</sup>, Kevin F. King<sup>4</sup>, Chris J. Hardy<sup>2</sup>, Luca Marinelli<sup>2</sup>, and Marion I. Menzel<sup>1</sup>

<sup>1</sup>GE Global Research, Garching, Germany, <sup>2</sup>GE Global Research, Niskayuna, NY, United States, <sup>3</sup>Technical University Munich, Garching, Germany, <sup>4</sup>GE Healthcare, Waukesha, WI, United States

**Introduction:** Diffusion spectrum imaging (DSI) [1], in which the diffusion encoding space ( $q$ -space) is Nyquist sampled, allows for resolving crossing fiber tracts in the brain or characterizing diffusional kurtosis [2]. Standard data processing in DSI is based on the magnitude of the data, while their phase is neglected. However, this phase contains clinically valuable information about coherent motion like flow or pulsatility [3]. Moreover, by separating the phase information from the data, subsequent processing like tensor fitting or fiber tracking can be done based on the real part of the data avoiding the bias introduced by the Rician noise distribution [4] of the magnitude data. This work presents a robust workflow for a phase sensitive reconstruction (PSR) of DSI data allowing for the extraction of velocity components and bias-free diffusion information. It may also be used/combined with other diffusion acquisition schemes in particular compressed-sensing-accelerated DSI [5].

**Theory:** Phase variations in DSI are essentially related to two effects: 1) magnetic field inhomogeneities and eddy currents (so called *background (BG) phase*, independent of the diffusion encoding) and 2) coherent motion during the acquisition. The latter is linearly dependent on the diffusion encoding direction and strength, i.e. on the  $q$ -space coordinate of the corresponding image and can be quantified using velocity encoding (VENC) [4].

**Methods:** The proposed PSR workflow consists of essentially five steps (cf. Fig. 1): First, the 6D MR raw data (3D  $k$ -space, 3D  $q$ -space) of the DSI scan is reconstructed into image space (*step 1*). Using standard inverse Fourier transform (in case of single coil data) or most parallel imaging techniques, the resulting diffusion weighted images (DWIs) are complex. Also advanced recon techniques like the recently proposed joint recon [6] can be employed provided that they yield complex output.

Due to the intrinsic wrapping of the phase into the  $[-\pi, \pi]$ -interval, unwrapping techniques are used to remove wraps in the phase images (*step 2*). The BG phase is removed by fitting (step 3) and subsequent subtraction of a polynomial from the phase maps. The order of the polynomial can be chosen fairly small ( $\leq 3$ ) due to the slowly varying character of the BG phase. In case of a 2D acquisition scheme like EPI, this should be done slice-by-slice using a 2D fitting approach.

For the remaining phase, the data for each image pixel is investigated independently in  $q$ -space: Linear fitting (3D, *step 4*) is performed, whereas the resulting three parameters characterize the coherent motion. The motion is quantified by computing directional velocity profiles based on the VENC of the DSI acquisition (*step 5*).

After subtracting the linear profiles from the phase data in  $q$ -space, the remaining phase can be treated as noise. Hence the real part of the data fully describes the diffusion data and subsequent data processing like tensor fitting or fiber tracking can be done based on the real data. If both fitting procedures (steps 3 & 4) are addressed in a least squares sense, no bias is introduced to the data.

DSI experiments on a healthy volunteer were performed using a 3T GE MR750 clinical MR scanner (GE Healthcare, Milwaukee, WI, USA) and a single Tx/Rx Head Coil ( $TE = 96$  ms,  $TR = 3$  s,  $128 \times 128$ ,  $FOV = 24$  cm) on a  $11^3$  cube ( $b_{max} = 2,000$  s/mm<sup>2</sup>). Step 1 was performed using standard EPI reconstruction. Step 2 was done using the *quality guided path following method* [7]. The fitting order in step 3 was set to 2. In step 5,  $VENC = 0.13$  mm/s (corresponding to the highest  $b$ -value) was used. Diffusion and kurtosis tensors were fitted based on the real valued DWIs and fractional anisotropy (FA) and mean kurtosis (MK) were evaluated.

**Results:** Fig. 2 depicts real part and phase of an example DWI as well as  $q$ -space phase maps and fitted FA and MK maps after the various data processing steps. Using the real data without BG phase correction yielded meaningless tensor metrics. However, after step 3 the linear relation of the phase in  $q$ -space becomes visible. After correcting for this phase (step 4), also the phase in the DWIs is flattened yielding real data that is close to the magnitude. Also FA and MK yield very reasonable results (except for the ventricles). Fig. 3 shows the velocity profiles obtained by step 5.

**Discussion:** PSR has been successfully applied to DSI data. Except for the ventricles, the phase has been nicely separated from the diffusion data. This proof of principle enables on the one hand (theoretically) bias free estimation of derived metrics like FA, kurtosis or fiber tracking and on the hand the analysis of flow/coherent motion in the brain.

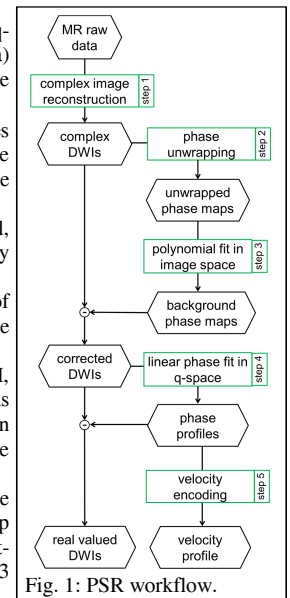


Fig. 1: PSR workflow.

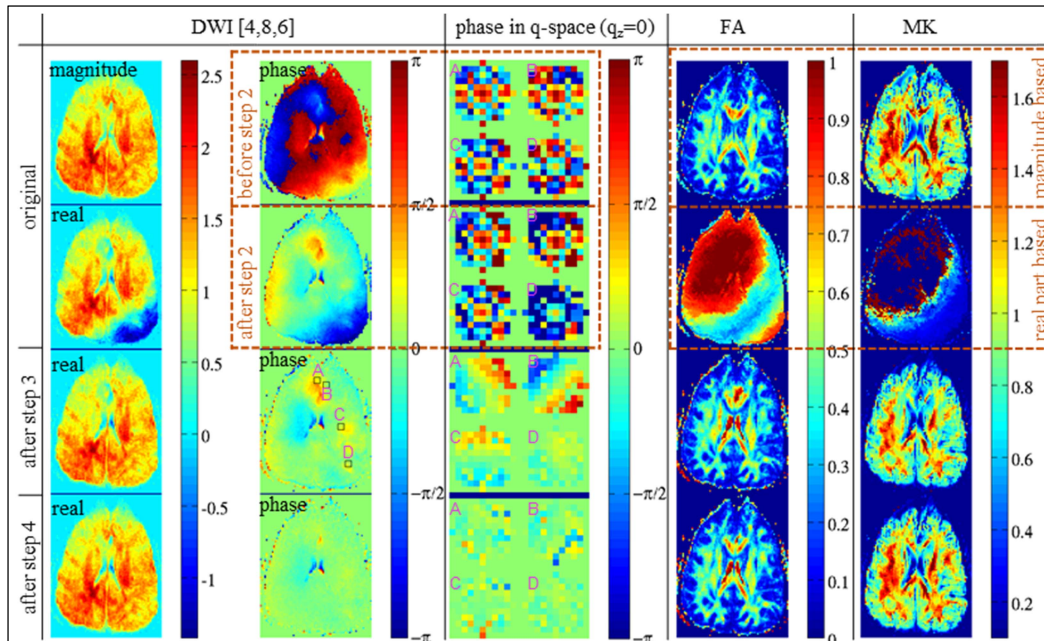


Fig. 2: DWI (col. 1&2), phase maps in  $q$ -space ( $q_x$ - $q_y$ -plane) for four example image pixels (col. 3) for different steps in the data processing (rows 1-4). FA (col. 4) and MK (col. 5) using the magnitude data (row 1) and using the real part of the data after the corresponding processing steps (rows 2-4).

## References:

- [1] Wedeen *et al.*, MRM 2005; 54(6)
- [2] Jensen *et al.*, MRM 2005; 53(6)
- [3] Soellinger *et al.*, MRM 2009; 61(1)
- [4] Cárdenas-Blanco *et al.*, Concepts Magn. Reson. Part A 2009
- [5] Menzel *et al.*, MRM 2011; 66(5)
- [6] Haldar *et al.*, MRM 2012
- [7] Ghiglia and Pritt, *John. Wiley & Sons, Inc.*, 1998

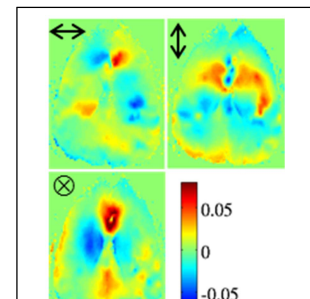


Fig. 3: Velocity profiles [mm/s] in the three spatial dimensions.